SpaceOps-2023, ID # 230

Venera-D multipurpose mission design

Vladislav A. Zubko [a,*], Natan A. Eismont [a], Andrey A. Belyaev [a], Konstantin S. Fedyaev [a], Lyudmila V. Zasova [a], Dmitriy A. Gorinov [a], Ravil R. Nazirov [a]

[a] *Space Research Institute of the Russian Academy of Sciences (IKI), 84/32 Profsoyuznaya Str, Moscow, 117997, Russia*
* Corresponding Author

Abstract

For a Venus exploration project, if it includes a lander, it is important to ensure landing in any desired site on the planet's surface. Due to the short duration of the launch window, traditionally assumed to be on the order of two weeks from the optimal launch date, it is very difficult to provide every point on the surface of Venus to be attainable for landing. In this research, a technique that allows to select and to reach any point on the surface of Venus as well as its application in the Venera-D project is considered. The basis of the proposed approach is the use of the Venus gravity assist maneuver to transfer the spacecraft to a resonant orbit having the same period as the Venus orbit with the subsequent return to the planet after 224.7 days and landing into the destination point. The total attainable landing areas for launch in 2029 and 2031 are provided. As a result of the research, it is shown that an application of the new approach allows to provide radical increase of attainable landing areas and also to provide access to any point on the surface of Venus with a small increase of characteristic velocity and flight duration.
Keywords: Venus, Venera-D, landing, attainable landing area, gravity assist maneuver, resonant orbit.

Introduction

Currently, several deep space research projects are being developed in Russia, such as ExoMars, Luna-25 (Luna-Globe) and Venera-D. The latter project is aimed at studying the surface and atmosphere of Venus using a lander and an orbital module. It is assumed that this mission to Venus will be carried out in several stages, the launch of which is planned during the launch windows in 2029-2031. The start of the first stage is scheduled for autumn 2029, and this stage is mainly to repeat the research mission of the Vega-1 and Vega-2 spacecraft. Subsequent stages will start later, their main scientific goal is to obtain and deliver samples of Venusian soil to the Earth.

One of the important problems in the Venera-D project focuses on the expansion of landing areas for the lander, i.e. enlarging sites attainable for landing under various constraints on the flight dynamics of the mission [1], [2]. Such problem arises due to possible inaccessibility of the desired landing sites which may be explained by range of reasons, such as peculiarities of the rotation dynamics of Venus, as well as possibilities of launching a spacecraft to the planet. These possibilities are limited by the repetition of favorable launch conditions (launch windows), i.e., when the flight to Venus requires the lowest cost of the characteristic velocity. Also, the attainable areas are influenced by restrictions on the orbiter trajectory. Finally landing sites are selected based on the surface features of the landing areas. Typically, the resulted attainable landing sites are reduced to only a few points on the Venus surface.

The main goal of the current research is to elaborate a method of expansion of landing sites on the Venus surface while satisfying all mentioned constraints and making almost all of the surface attainable for landing. The proposed method is based on the use of the gravitational field of Venus and the transfer of the spacecraft after the flyby of Venus to a heliocentric orbit with a period equal to the period of Venus revolution around the Sun (i.e., to an orbit resonant with the orbit of Venus in a ratio of 1:1). As a result, after a complete revolution in such an orbit, at the next approach to Venus, the lander will already be over another part of its surface, which will allow landing in a previously inaccessible area. Since the direction of the flyby of Venus at the first approach can be chosen arbitrarily, there is a bunch of possible 1:1 resonant orbits (mentioned above) which allows access to almost any point on the planet's surface. Notice, these possible resonant orbits are virtual in the meaning of a real flight, and one of the orbits should be selected in order to provide landing to the desired area of the surface. Of course, after the Venus flyby the spacecraft will move along the selected orbit, which cannot be changed during the flight.

Results of the research showed that the proposed strategy provides an essential extension of attainable landing areas and makes any point on Venus surface accessible with a small increasing ΔV required for launch from the Earth and, possibly, a small increasing of the flight duration. It should be noted that, of course, enlarging in the attainable landing areas will be accompanied with growth in total complexity of the mission as well as increasing duration between the launch and the landing stage. But at the same time the proposed approach may be the only way

to provide an access to previously unattainable areas, so the importance of consideration of this approach is beyond the doubts.

2. Mathematical methods used in the research

The considered flight to Venus, including gravity assist maneuver and motion along the resonant orbit, includes the following stages [7]–[9]:

(I) the stage of spacecraft flight from the Earth to Venus;

(II) gravitational maneuver near Venus, transferring the spacecraft to the heliocentric orbit resonant with the orbit of Venus;

(III) flight along the resonant orbit (with a ratio of periods of 1:1) until the next approach to Venus;

(IV) repeated approach to Venus with subsequent landing on its surface.

To calculate trajectory of the spacecraft between each pair of celestial bodies, we consider using the patched conic section method. In the framework of the method of patched conic the calculation of the trajectory of the spacecraft motion in the gravitational field of n celestial bodies is reduced to n two-body problems, the solution of each of them is a Keplerian orbit (i.e. a conic section) [3]. The problem is to find these Keplerian orbits and join them (patch them together) into a trajectory of the flight.

Determination of the heliocentric arcs between each pair of celestial bodies is carried out by solving the Lambert problem, which is to find the orbit by two positions and the transit time between them.

Notice, due to the specifics of the problem considered in this paper, the complete heliocentric trajectory of the flight from the Earth to Venus can be represented as a composition of two different flight segments: Earth-Venus and Venus-Venus. Flight between two consecutive approaches of the spacecraft to Venus occurs on a resonant orbit. In this case, the flight trajectory on the first section will be determined from the solution of the Lambert problem, and on the second segment the trajectory will be determined by the technique proposed in this paper.

Let us consider the near-Venus section of the flight after the second approach to Venus. At an entry into the Venusian sphere of influence one vector of the asymptotic velocity of the spacecraft corresponds to a bunch of approach hyperbolic trajectories. The intersection of this bunch of trajectories with the Venusian surface forms a landing circle. The angular radius of such a circle can be defined as follow [4], [5]:

$$\psi = \vartheta_{Entry} + \varphi, \tag{1}$$

where ϑ_{Entry} is the true anomaly of the spacecraft at the point of re-entry, deg; φ is the angular radius of the circle of possible pericenters, which is defined as follows:

$$\varphi = \arccos\left(\frac{\mu_{pl}}{\mu_{pl} + r_\pi V_r^{\,2}}\right), \tag{2}$$

where $r_\pi = r_\pi(\theta)$ is the radius of the imaginary pericenter, which depends on the entry angle (θ) of the spacecraft into the planet's atmosphere; V_r is the asymptotic velocity of the spacecraft; μ_{pl} is the gravitational parameter of the planet.

3. The optimization problem criteria and determination of the launch windows for a mission to Venus

The trajectory optimization criterion for the considered approach can be written as:

$$F_1 = F(t_o, t_k) = \Delta V_0(t_o, t_1) + V_r(t_1) + \Delta V_2(t_1, t_k), \tag{3}$$

where ΔV_0 is the launch characteristic velocity on the Earth-Venus arc of the trajectory; ΔV_2 is the characteristic velocity consumption on the Venus-Venus arc; V_r is the asymptotic velocity of the spacecraft at Venus; t_o, t_1, t_k are times of the launch, the planet flyby and the landing on the planet's surface, respectively.

The solution of the problem under consideration consists of the search for such trajectories, for which $\Delta V_2(t_1, t_k) = 0$. This is possible due to the existence of at least one solution, at which the spacecraft transfers to a resonant 1:1 orbit.

The isolines plotted for the criterion (3) as a function of the launch and arrival dates are shown in Fig. 1.

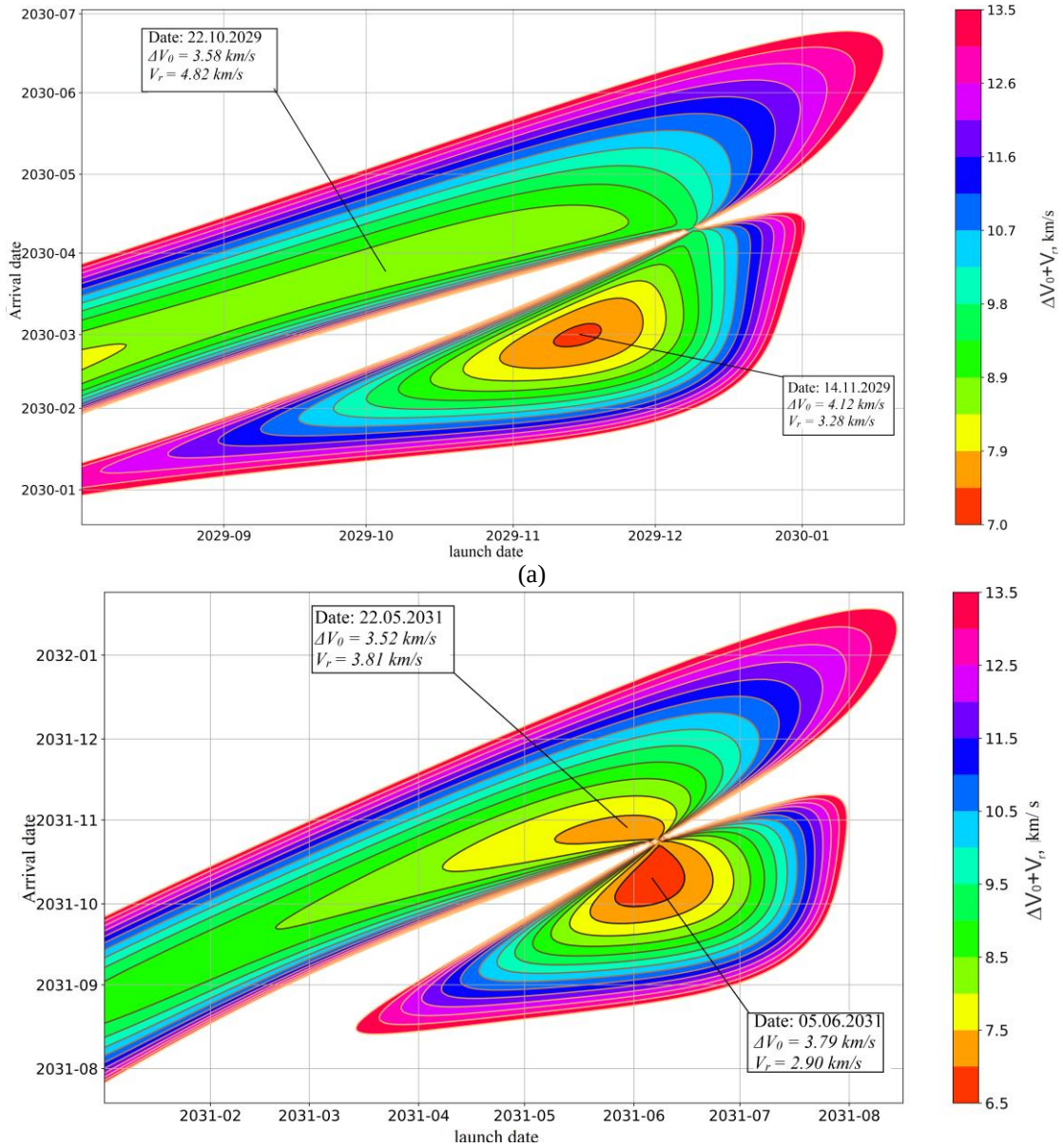

Fig.1. The value of ΔV_0+V_r as a function of the launch and arrival dates for launch windows in (a) 2029; (b) 2031

Let us write out from Fig. 3 the optimal launch dates of flight from Earth to Venus by criterion (3), and some basic parameters: ΔV_0, V_r, α^* in Table 1.

Table 1. Optimal launch dates, as well as some basic parameters for a flight to Venus

1st semi-turn				2nd semi-turn			
Optimal launch date	ΔV_0, km/s	V_r, km/s	α^*, deg	Optimal launch date	ΔV_0, km/s	V_r, km/s	α^*, deg
14.11.2029	4.12	3.28	108.0	22.10.2029	3.58	4.82	85.77
05.06.2031	3.79	2.90	127.0	22.05.2031	3.52	3.81	100.98

4. Attainable landing areas for launch in 2029 and 2031

Fig. 4 shows inaccessible for landing areas on the surface of Venus for a flight within one launch/arrival date (darkened areas), also areas completely inaccessible for landing (yellow, shaded areas) are shown.

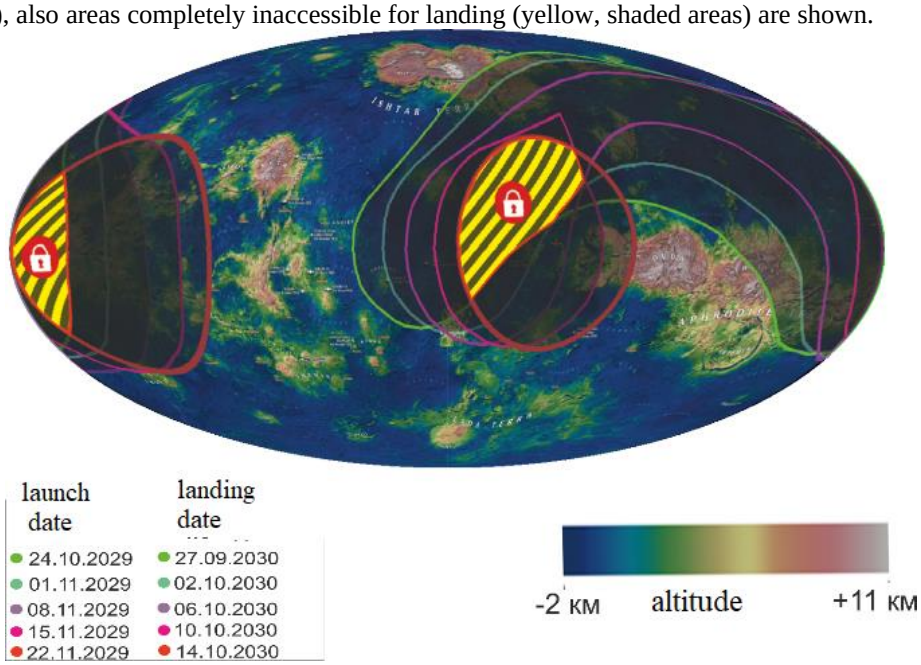

(a)

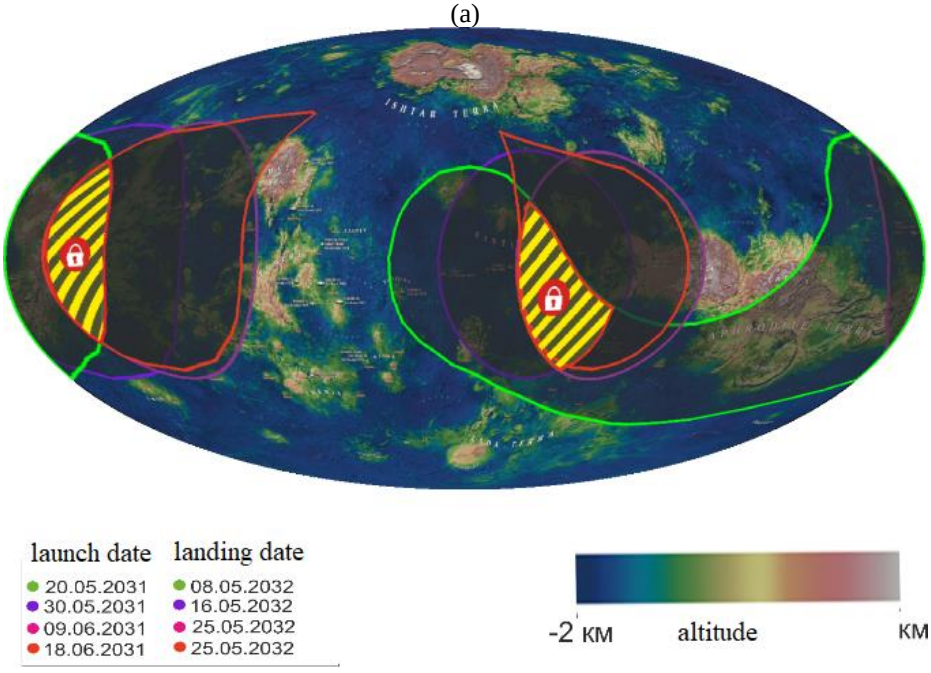

(b)

Fig. 2. Regions unattainable for landing (for the given date of arrival, darkened on the figure) and their movement on the surface of Venus in the launch window (a) in 2029; (b) in 2031. Note: Yellow shaded areas show areas completely unattainable for landing. Areas are built on the map of Venus in the equiplanar projection Mollweide, the central meridian is aligned with the zero for Venus (Alpha Regio).

In Fig. 3 it is shown that due to the superposition of reachable landing areas, obtained in one pair of launch/landing dates, it is possible to exclude unattainable areas and reduce the influence of limitations arising from the accepted

angle of entry into the atmosphere. Note that when the entry angle of 34.5 degrees is selected, the entire surface of Venus becomes accessible as it is shown in the research [7].

3. Construction of attainable landing areas considering the orbiter requirements

Currently, only one mission is known to send both a landing vehicle and an orbital module - Venera-D [1]. Scheme of spacecraft flight in the sphere of influence of Venus within the framework of the Venera-D mission is assumed as follows: the spacecraft approaching Venus in three days is separates to lander and orbiter, then the orbiter and lander by loop scheme approach Venus, the orbital module goes to near-Venus orbit with pericenter at 500 km height [1] (Fig. 3).

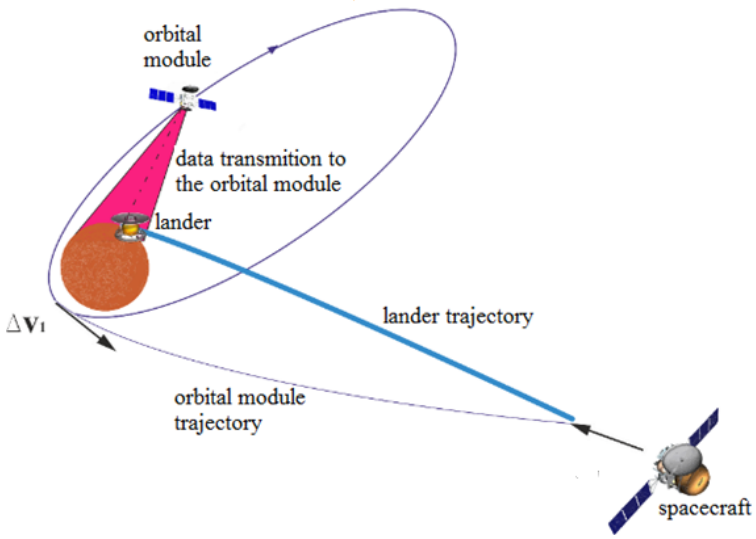

Fig. 3. Scheme of landing on the surface of Venus (ΔV_1 - braking impulse applied to the spacecraft to enter the orbit of the artificial satellite of Venus).

Let us consider the restrictions imposed on the orbiter trajectory within the current mission design:

- Costs of characteristic velocity for the orbiter to break into the planetocentric orbit should not exceed 1700 m/s.
- Ensuring visibility between the lander and the orbiter during all phases of descent and for several hours after landing.
- The duration of the satellite in orbit should not be less than 8 years.
- Duration of occultation events should not exceed 60 min.

Note that the first requirement is best satisfied for orbits with a period of 1 day [1]. A detailed example of building a trajectory with a landing vehicle and an orbital module was considered in [1]. In this paper we presenting the results of calculation of total unattainable areas (yellow zones on map fig. 4) obtained considering the above mentioned restrictions to orbiter for landing in 2030 and 2033 (launch in 2029 and 2032, i.e. in the most likely launch windows for the Venera-D mission).

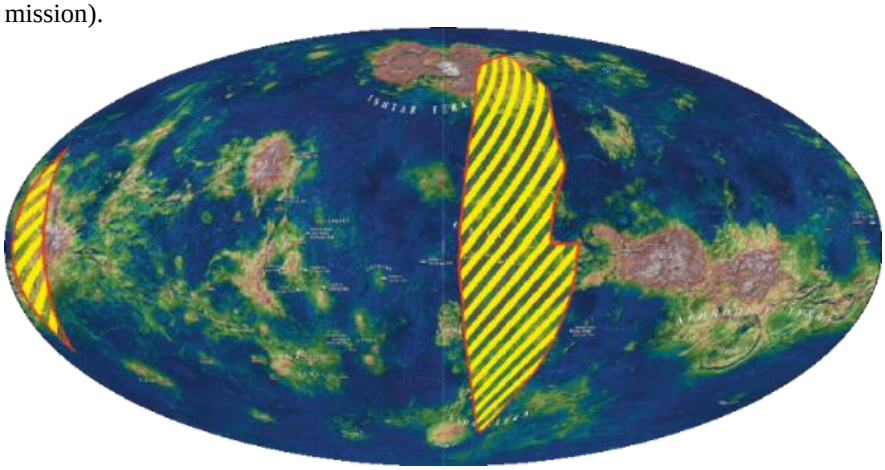

(a)

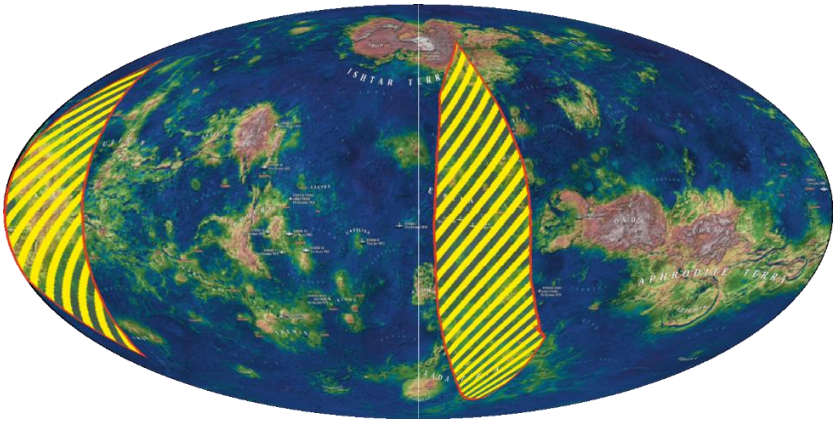

(b)

Fig. 4 The total unattainable landing areas (yellow zones) for probe landing in 2030 (a) and 2032 (b) corresponding to 2029 and 2031 launch window. The areas are built on the map of Venus in the Mollweide projection, the central meridian is aligned with the zero for Venus (area of the region Alpha).

As can be seen from the above figures, due to the restrictions imposed for the orbiter, from the attainable areas shown in the previous section (Fig. 2) will be "cut out" some areas.

4. Comparing the proposed technique to the known ones

At the moment we can distinguish several approaches, relatively uncomplicated, which are well known in the literature [10], and also are widely used in the design of interplanetary missions including a landing stage (i.e. descent from a planet-centric intermediate orbit). Let us list the main approaches to extend the landing regions, which our approach is supposed to be compared with:

1. extension of the launch window;
2. landing performed from the elliptical orbit of a satellite of the planet;
3. use of a special form of the lander.

In the first approach some expansion in the attainable landing areas may be achieved by enlarging the launch window resulted in increase in characteristic velocity.

The second approach involves breaking into an intermidiate elleptical orbit with a further landing in the vicinity of the pericenter. Note that in the best scenario the intermediate orbit should be chosen circular, because in this case the spacecraft needs to wait no more than 243 days (in the case of Venus) to perform landing at the required point. In the case of an elliptical orbit, in addition to coincidence of longitudes, the pericenter of the orbit is required to be in the vicinity of the landing point latitudes. Note that this approach is extremely "expensive" in terms of the required characteristic velocity spent on braking to the intermediate orbit. Moreover, the closer the final orbit is to the circular one, the higher is the price of such an approach.

The third approach is based on the use of technical (aerodynamic) properties of the landing vehicle. If for the previously described approaches the shape of the lander did not play a significant role and in the simplest case it was assumed to be spherical, for this approach it is proposed to use such a shape, which will provide high maneuverability of the lander in the dense Venusian atmosphere and allow to control lander during descent, thereby expanding the attainable areas for landing. Details on this approach can be found in the works [11], [12].

Here is a qualitative comparison of the approach discussed in this study and the already existing techniques (Table 2). Note that the data given in Table 3 are estimates obtained by the authors during numerous modeling of various approaches of expansion of landing capabilities in a given region on the surface of Venus.

Table 2. Qualitative comparison of the proposed technique with already existing ones

	Landing directly from the Earth-Venus interplanetary trajectory	Extension launch window	Landing from an elliptical (circular) orbit of a satellite of Venus	Using complex aerodynamically shaped lander to control descent in the Venusian	Proposed approach to the construction of flight trajectories with gravity assist maneuver and

				atmosphere	subsequent flight on a resonant orbit
Increaing ΔV_0	less than 100 m/s	high (300 m/s or more)	less than 100 m/s	less than 100 m/s	less than 100 m/s
Specific requirements for the design of the lander	not reqired	not reqired	not reqired	Special aerodynamic shape required	not reqired
Costs of orbital maneuvers to reach the landing point	not reqired	not reqired	high (more than 1 km/s)	not reqired	not reqired
Percentage of available Venus surface areas for the date of arrival	<5%	15%-25%	75-100%	~40-50%	70-100%
ΔT	~1 days	~1 days	to 243 days	~1 days	~224.7 days

*ΔT - Duration of reaching the given landing point (counted from the moment of approach to the Venus sphere of influence).
** In the table the advantages (green color gradient) and disadvantages (red gradient) of this or that approach to the construction of trajectories of the flight to a given point on the surface of Venus are highlighted with color.

5. Conclusions

As a result of the study it is shown that the use of the proposed approach to the construction of trajectories of flight to Venus, using the gravity assist maneuver and a flight on a resonant orbit leads to a radical expansion of the attainable areas of landing.

To demonstrate the potential for expanding attainable landing areas, maps showing the available landing area of Venus using the proposed approach for launch windows in 2029 and 2031 have been drawn out.

Also, the discussed technique was applied in the framework of the Venera-D scenario. The proposed approach showed its effectiveness even in such complex scenario as for the Venera-D mission.

References

[1] N. A. Eismont *et al.*, Venera-D Mission Scenario and Trajectory, *Sol. Syst. Res.*, vol. 53, no. 7, pp. 578–585, 2019, doi: 10.1134/S0038094619070062.
[2] M. A. Ivanov, L. Zasova, and T. K. P. Gregg, Venera-D Landing Site Constraints, in *The Ninth Moscow Solar System Symposium 9M-S3*, 2018, pp. 58–59.
[3] A. PRADO, A comparison of the ‘patched-conics approach’ and the restricted problem for swing-bys, *Adv. Sp. Res.*, vol. 40, no. 1, pp. 113–117, 2007, doi: 10.1016/j.asr.2007.01.012.
[4] D. A. Vallado, FUNDAMENTALS OF ASTRODYNAMICS AND APPLICATIONS, *J. Chem. Inf. Model.*, vol. 53, no. 9, 2016.
[5] N. Eismont *et al.*, Expansion of landing areas on the Venus surface using resonant orbits in the Venera-D project, *Acta Astronaut.*, vol. 197, pp. 310–322, Mar. 2022, doi: 10.1016/j.actaastro.2022.03.014.
[6] B. A. Archinal *et al.*, Report of the IAU Working Group on Cartographic Coordinates and Rotational Elements: 2009, *Celest. Mech. Dyn. Astron.*, vol. 109, no. 2, 2011, doi: 10.1007/s10569-010-9320-4.
[7] N. Eismont *et al.*, Expansion of landing areas on the Venus surface using resonant orbits in the Venera-D project, *Acta Astronaut.*, vol. 197, pp. 310–322, Aug. 2022, doi: 10.1016/j.actaastro.2022.03.014.
[8] N. A. Eismont *et al.*, Gravity assists maneuver in the problem of extension accessible landing areas on the Venus surface, *Open Astron.*, vol. 30, no. 1, pp. 103–109, 2021, doi: 10.1515/astro-2021-0013.
[9] N. A. Eismont *et al.*, Resonant Orbits in the Problem of Expanding the Reachable Landing Areas on the Surface of Venus, *Astron. Lett.*, vol. 47, no. 5, pp. 316–330, 2021, doi: 10.1134/S1063773721050042.
[10] N. A. Eismont, V. Koryanov, K. S. Fedyaev, S. A. Bober, V. A. Zubkov, and A. A. Belyaev, On the possibility of expanding the landing areas within the VENERA-D project by selecting launch windows, in *AIP Conference Proceedings*, 2021, vol. 2318, doi: 10.1063/5.0037426.
[11] A. V. Kosenkova, Investigation of reachable landing sites in the VENERA-D mission for various types of a lander, in *AIP Conference Proceedings*, 2021, vol. 2318, doi: 10.1063/5.0035839.

[12] A. Kosenkova and V. Minenko, Investigation of various lander's configurations possibilities capable of maneuvering descent to the Venus surface, in *Proceedings of the International Astronautical Congress, IAC*, 2020, vol. 2020-October.

Appendix A. Tables of the trajectory parameters for the 2029-2031 launch windows

The tables show the dates of launch, flyby and landing on the surface of Venus, as well as the required ΔV of launch, flyby speed and orientation parameters of the vector of asymptotic velocity of the spacecraft near Venus. The tables also contain data on the required angles of rotation of the vector of arrival asymptotic velocity and on the achievable angles. Note that in all cases where $\alpha^* < \alpha_{max}$ is available for selection any of the resonant orbits from the 1:1 manifold.

Trajectories are conventionally divided into the first semi-turn, in which the part of the spacecraft trajectory from Earth to Venus occurs at flight angles of less than 180 degrees, and the second semi-turn (flight angle exceeds 180 degrees).

Table A.1 Characteristics of the 2029 Venus mission (first semi-turn trajectories)

Launch date	Flyby date	Landing date	α_{min}, deg.	α_{max}, deg.	α^*, deg.	δ, deg.	ΔV_0, km/s	V_r, km/s	$\Delta V_0 + V_r$, km/s
01.11.2029	19.02.2030	02.10.2030	44.36	141.97	100.06	48.81	3.92	3.89	7.80
02.11.2029	20.02.2030	03.10.2030	45.53	140.71	101.02	47.59	3.93	3.83	7.76
03.11.2029	21.02.2030	03.10.2030	46.74	139.40	101.96	46.33	3.94	3.77	7.71
04.11.2029	21.02.2030	04.10.2030	48.01	138.05	102.89	45.02	3.95	3.72	7.67
05.11.2029	22.02.2030	04.10.2030	49.32	136.66	103.78	43.67	3.96	3.67	7.62
06.11.2029	22.02.2030	05.10.2030	50.67	135.22	104.65	42.27	3.97	3.61	7.59
07.11.2029	23.02.2030	06.10.2030	52.08	133.73	105.49	40.83	3.98	3.57	7.55
08.11.2029	23.02.2030	06.10.2030	53.53	132.21	106.29	39.34	4.00	3.52	7.52
09.11.2029	24.02.2030	07.10.2030	55.02	130.65	107.05	37.82	4.01	3.48	7.49
10.11.2029	25.02.2030	07.10.2030	56.55	129.05	107.77	36.25	4.03	3.43	7.46
11.11.2029	25.02.2030	08.10.2030	58.11	127.43	108.43	34.66	4.04	3.40	7.44
12.11.2029	26.02.2030	08.10.2030	59.71	125.77	109.05	33.03	4.06	3.36	7.42
13.11.2029	26.02.2030	09.10.2030	61.33	124.10	109.60	31.39	4.08	3.33	7.41
14.11.2029	27.02.2030	10.10.2030	62.96	122.42	110.09	29.73	4.10	3.30	7.40
15.11.2029	28.02.2030	10.10.2030	64.61	120.74	110.52	28.07	4.12	3.28	7.40
16.11.2029	28.02.2030	11.10.2030	66.25	119.07	110.88	26.41	4.14	3.26	7.40
17.11.2029	01.03.2030	11.10.2030	67.87	117.43	111.16	24.78	4.17	3.24	7.41
18.11.2029	01.03.2030	12.10.2030	69.45	115.82	111.37	23.19	4.19	3.23	7.43
19.11.2029	02.03.2030	13.10.2030	70.97	114.29	111.49	21.66	4.22	3.23	7.45
20.11.2029	02.03.2030	13.10.2030	72.41	112.85	111.54	20.22	4.25	3.22	7.47
21.11.2029	03.03.2030	14.10.2030	73.72	111.54	111.49	18.91	4.28	3.23	7.50
22.11.2029	04.03.2030	14.10.2030	74.88	110.40	111.36	17.76	4.31	3.23	7.54
23.11.2029	04.03.2030	15.10.2030	75.83	109.47	111.14	16.82	4.34	3.25	7.59
24.11.2029	05.03.2030	15.10.2030	76.52	108.80	110.83	16.14	4.38	3.26	7.64
25.11.2029	05.03.2030	16.10.2030	76.91	108.45	110.43	15.77	4.41	3.28	7.70
26.11.2029	06.03.2030	17.10.2030	76.97	108.44	109.92	15.74	4.45	3.31	7.76
27.11.2029	07.03.2030	17.10.2030	76.65	108.81	109.32	16.08	4.49	3.35	7.83
28.11.2029	07.03.2030	18.10.2030	75.98	109.55	108.61	16.79	4.53	3.39	7.91
01.11.2029	19.02.2030	02.10.2030	44.36	141.97	100.06	48.81	3.92	3.89	7.80
02.11.2029	20.02.2030	03.10.2030	45.53	140.71	101.02	47.59	3.93	3.83	7.76

Table A.2 Characteristics of the 2029 Venus mission (second semi-turn trajectories)

Launch date	Flyby date	Landing date	α_{min}, deg.	α_{max}, deg.	α^*, deg.	δ, deg.	ΔV_0, km/s	V_r, km/s	$\Delta V_0 + V_r$, km/s
12.10.2029	29.03.2030	09.11.2030	32.79	155.10	86.02	61.16	3.62	4.81	8.43
13.10.2029	29.03.2030	09.11.2030	32.70	155.19	85.99	61.25	3.62	4.81	8.43

14.10.2029	30.03.2030	09.11.2030	32.61	155.28	85.96	61.34	3.61	4.81	8.42
15.10.2029	30.03.2030	10.11.2030	32.52	155.37	85.94	61.42	3.61	4.81	8.42
16.10.2029	31.03.2030	10.11.2030	32.44	155.46	85.91	61.51	3.60	4.81	8.42
17.10.2029	31.03.2030	11.11.2030	32.36	155.54	85.89	61.59	3.60	4.82	8.42
18.10.2029	31.03.2030	11.11.2030	32.29	155.62	85.87	61.67	3.60	4.82	8.41
19.10.2029	01.04.2030	11.11.2030	32.21	155.70	85.84	61.74	3.59	4.82	8.41
20.10.2029	01.04.2030	12.11.2030	32.14	155.78	85.82	61.82	3.59	4.82	8.41
21.10.2029	02.04.2030	12.11.2030	32.07	155.85	85.80	61.89	3.59	4.82	8.41
22.10.2029	02.04.2030	13.11.2030	32.00	155.92	85.77	61.96	3.58	4.82	8.41
23.10.2029	02.04.2030	13.11.2030	31.94	155.99	85.75	62.02	3.58	4.83	8.41
24.10.2029	03.04.2030	14.11.2030	31.87	156.05	85.72	62.09	3.58	4.83	8.41
25.10.2029	03.04.2030	14.11.2030	31.81	156.12	85.70	62.15	3.58	4.83	8.41
26.10.2029	04.04.2030	14.11.2030	31.76	156.18	85.67	62.21	3.58	4.83	8.41
27.10.2029	04.04.2030	15.11.2030	31.70	156.24	85.64	62.27	3.58	4.83	8.41
28.10.2029	04.04.2030	15.11.2030	31.65	156.30	85.61	62.32	3.58	4.84	8.42
29.10.2029	05.04.2030	15.11.2030	31.59	156.35	85.58	62.38	3.58	4.84	8.42
30.10.2029	05.04.2030	16.11.2030	31.54	156.41	85.55	62.43	3.58	4.84	8.42
31.10.2029	06.04.2030	16.11.2030	31.50	156.46	85.51	62.48	3.58	4.84	8.43
01.11.2029	06.04.2030	17.11.2030	31.45	156.51	85.47	62.53	3.59	4.85	8.43
02.11.2029	06.04.2030	17.11.2030	31.41	156.56	85.43	62.57	3.59	4.85	8.44
03.11.2029	07.04.2030	17.11.2030	31.37	156.60	85.39	62.62	3.59	4.85	8.45
04.11.2029	07.04.2030	18.11.2030	31.33	156.65	85.34	62.66	3.60	4.86	8.45
05.11.2029	07.04.2030	18.11.2030	31.29	156.69	85.29	62.70	3.60	4.86	8.46
06.11.2029	08.04.2030	18.11.2030	31.26	156.74	85.23	62.74	3.61	4.86	8.47
07.11.2029	08.04.2030	19.11.2030	31.22	156.78	85.17	62.78	3.61	4.87	8.48
08.11.2029	08.04.2030	19.11.2030	31.19	156.82	85.11	62.81	3.62	4.87	8.49
09.11.2029	09.04.2030	19.11.2030	31.16	156.85	85.04	62.85	3.62	4.88	8.50
10.11.2029	09.04.2030	20.11.2030	31.14	156.89	84.96	62.88	3.63	4.88	8.51

Table A.3 Characteristics of the 2031 Venus mission (first semi-turn trajectories)

Launch date	Flyby date	Landing date	α_{min}, deg.	α_{max}, deg.	α^*, deg.	δ, deg.	ΔV_0, km/s	V_r, km/s	$\Delta V_0 + V_r$, km/s
20.05.2031	26.09.2031	08.05.2032	49.30	136.72	103.69	43.71	3.82	3.67	7.49
21.05.2031	27.09.2031	08.05.2032	50.92	134.97	104.97	42.02	3.82	3.60	7.41
22.05.2031	28.09.2031	09.05.2032	52.63	133.14	106.24	40.25	3.81	3.52	7.33
23.05.2031	28.09.2031	10.05.2032	54.44	131.21	107.47	38.39	3.81	3.45	7.26
24.05.2031	29.09.2031	11.05.2032	56.34	129.20	108.68	36.43	3.80	3.38	7.19
25.05.2031	30.09.2031	12.05.2032	58.35	127.08	109.84	34.37	3.80	3.32	7.12
26.05.2031	01.10.2031	12.05.2032	60.46	124.87	110.96	32.21	3.80	3.26	7.05
27.05.2031	02.10.2031	13.05.2032	62.67	122.56	112.02	29.95	3.79	3.20	6.99
28.05.2031	02.10.2031	14.05.2032	64.99	120.15	113.01	27.58	3.79	3.14	6.93
29.05.2031	03.10.2031	15.05.2032	67.42	117.64	113.93	25.11	3.79	3.09	6.88
30.05.2031	04.10.2031	16.05.2032	69.96	115.03	114.77	22.54	3.79	3.05	6.84
31.05.2031	05.10.2031	17.05.2032	72.59	112.33	115.52	19.87	3.79	3.01	6.79
01.06.2031	06.10.2031	18.05.2032	75.32	109.54	116.16	17.11	3.79	2.97	6.76
02.06.2031	07.10.2031	18.05.2032	78.11	106.70	116.69	14.29	3.79	2.94	6.73
03.06.2031	08.10.2031	19.05.2032	80.95	103.83	117.09	11.44	3.79	2.92	6.71
04.06.2031	09.10.2031	20.05.2032	83.73	101.03	117.36	8.65	3.79	2.91	6.70
05.06.2031	09.10.2031	21.05.2032	86.23	98.51	117.48	6.14	3.79	2.90	6.69
06.06.2031	10.10.2031	22.05.2032	87.81	96.94	117.45	4.56	3.79	2.90	6.70
07.06.2031	11.10.2031	23.05.2032	87.39	97.37	117.26	4.99	3.79	2.91	6.71
08.06.2031	12.10.2031	24.05.2032	85.40	99.39	116.91	6.99	3.80	2.93	6.73
09.06.2031	13.10.2031	25.05.2032	83.03	101.80	116.44	9.39	3.80	2.96	6.76

10.06.2031	13.10.2031	25.05.2032	80.86	104.02	115.88	11.58	3.81	2.99	6.80
11.06.2031	14.10.2031	25.05.2032	79.14	105.78	115.31	13.32	3.82	3.02	6.84
12.06.2031	14.10.2031	25.05.2032	77.87	107.10	114.76	14.61	3.83	3.05	6.88
13.06.2031	14.10.2031	25.05.2032	76.90	108.13	114.23	15.61	3.85	3.08	6.92
14.06.2031	14.10.2031	25.05.2032	76.09	108.98	113.70	16.44	3.86	3.10	6.97
15.06.2031	14.10.2031	25.05.2032	75.37	109.75	113.16	17.19	3.88	3.13	7.02
16.06.2031	13.10.2031	25.05.2032	74.72	110.45	112.62	17.87	3.90	3.16	7.07
17.06.2031	13.10.2031	25.05.2032	74.09	111.12	112.05	18.52	3.93	3.20	7.12
18.06.2031	13.10.2031	25.05.2032	73.49	111.78	111.47	19.15	3.95	3.23	7.18

Table A.4 Characteristics of the 2031 Venus mission (second semi-turn trajectories)

Launch date	Flyby date	Landing date	α_{min}, deg.	α_{max}, deg.	α^*, deg.	δ, deg.	ΔV_0, km/s	V_r, km/s	$\Delta V_0 + V_r$, km/s
09.05.2031	23.10.2031	04.06.2032	44.05	142.46	98.32	49.20	3.51	3.99	7.51
10.05.2031	24.10.2031	04.06.2032	44.17	142.33	98.51	49.08	3.51	3.98	7.49
11.05.2031	24.10.2031	05.06.2032	44.29	142.18	98.70	48.95	3.51	3.97	7.48
12.05.2031	24.10.2031	05.06.2032	44.42	142.04	98.90	48.81	3.51	3.96	7.47
13.05.2031	24.10.2031	05.06.2032	44.56	141.88	99.09	48.66	3.51	3.95	7.45
14.05.2031	25.10.2031	05.06.2032	44.70	141.71	99.29	48.51	3.51	3.94	7.44
15.05.2031	25.10.2031	05.06.2032	44.85	141.54	99.49	48.34	3.51	3.92	7.43
16.05.2031	25.10.2031	06.06.2032	45.01	141.36	99.69	48.17	3.51	3.91	7.42
17.05.2031	25.10.2031	06.06.2032	45.19	141.17	99.90	47.99	3.51	3.90	7.41
18.05.2031	25.10.2031	06.06.2032	45.37	140.97	100.11	47.80	3.51	3.89	7.39
19.05.2031	25.10.2031	06.06.2032	45.56	140.76	100.32	47.60	3.51	3.87	7.38
20.05.2031	26.10.2031	06.06.2032	45.76	140.53	100.53	47.39	3.51	3.86	7.37
21.05.2031	26.10.2031	06.06.2032	45.97	140.30	100.75	47.16	3.51	3.85	7.36
22.05.2031	26.10.2031	07.06.2032	46.20	140.05	100.98	46.92	3.52	3.83	7.35
23.05.2031	26.10.2031	07.06.2032	46.44	139.78	101.20	46.67	3.52	3.82	7.34
24.05.2031	26.10.2031	07.06.2032	46.70	139.50	101.44	46.40	3.52	3.80	7.33
25.05.2031	26.10.2031	07.06.2032	46.98	139.20	101.68	46.11	3.52	3.79	7.32
26.05.2031	26.10.2031	07.06.2032	47.28	138.88	101.93	45.80	3.53	3.78	7.30
27.05.2031	26.10.2031	07.06.2032	47.60	138.53	102.19	45.47	3.53	3.76	7.29
28.05.2031	26.10.2031	07.06.2032	47.94	138.16	102.45	45.11	3.54	3.74	7.28
29.05.2031	26.10.2031	07.06.2032	48.32	137.76	102.73	44.72	3.55	3.73	7.27
30.05.2031	26.10.2031	07.06.2032	48.73	137.32	103.03	44.30	3.55	3.71	7.26
31.05.2031	26.10.2031	07.06.2032	49.18	136.84	103.34	43.83	3.56	3.69	7.25
01.06.2031	26.10.2031	07.06.2032	49.68	136.31	103.68	43.32	3.57	3.67	7.24
02.06.2031	26.10.2031	07.06.2032	50.23	135.72	104.04	42.74	3.58	3.65	7.23
03.06.2031	26.10.2031	07.06.2032	50.87	135.05	104.44	42.09	3.59	3.63	7.22
04.06.2031	26.10.2031	07.06.2032	51.59	134.28	104.89	41.34	3.60	3.60	7.20
05.06.2031	26.10.2031	06.06.2032	52.45	133.37	105.41	40.46	3.62	3.57	7.19
06.06.2031	25.10.2031	06.06.2032	53.49	132.27	106.02	39.39	3.64	3.54	7.17
07.06.2031	25.10.2031	05.06.2032	54.83	130.86	106.78	38.01	3.66	3.49	7.15